Nature Environment and Pollution Technology
An International Quarterly Scientific Journal

p-ISSN: 0972-6268
(Print copies up to 2016)
e-ISSN: 2395-3454

Vol. 25 | No. 3 | Article ID B4389 | 2026

Original Research Paper

https://doi.org/10.46488/NEPT.2026.v25i03.B4389

Open Access Journal

Thermogravimetric Analysis and Determination of Kinetic Parameters for Pyrolysis of Lotus Seed Biomass

Gurneet Kaur[1], Vivekanand[2] and Jaibir Kherb[3]†

[1]Department of Chemistry, Amity Institute of Applied Sciences, Amity University, Noida-201301, India
[2]Department of Chemistry, Govind Ballabh Pant University of Agriculture & Technology, Pantnagar, Udham Singh Nagar, Uttarakhand 263145, India
[3]Department of Chemistry, National Institute of Technology, Kurukshetra-136119, Haryana, India
†Corresponding author: Jaibir Kherb; jaibirkherb@nitkkr.ac.in

Abbreviation: Nat. Env. & Poll. Technol.
Website: www.neptjournal.com

Received: 11-08-2025
Revised: 23-10-2025
Accepted: 26-10-2025

Key Words:

Biomass pyrolysis
Thermogravimetric analysis
Thermokinetic modeling
Lotus seed biomass

ABSTRACT

Optimal usage of omnipresent biowaste materials is vital for truly accomplishing global sustainable development goals. In this regard, naturally abundant, nutrient-rich lotus seeds (Nelumbo nucifera) biomass holds high potential as a suitable alternative source of energy. This research systematically investigates the high temperature thermochemical, morphological and spectral changes which occur in lotus seeds (LS) biomass. This study also successfully correlates the thermogravimetric changes in LS biomass with its compositional changes, highlighting the overall mechanism of this thermal process. Furthermore, a detailed theoretical analysis of the thermal data was also carried out using various models to obtain all of the involved kinetic parameters. Results showed that LS biomass thermal degradation followed a first-order reaction kinetics mechanism with significantly low activation energy requirements (~ 2-8 $kJ.mol^{-1}$) for different reaction phases. These results provide critical information for optimizing the energy production on an industrial scale. High volatile content (~76%) and lower pyrolysis temperature requirement (< 400°C) for inducing significant structural changes in this biomass also enhances its potential as a bioenergy alternative. Ultimately, this research work underscores the potential of lotus seed biomass to contribute to sustainable energy solutions and mitigate environmental pollution, aligning with global efforts toward renewable energy practices.

Citation for the Paper:

Kaur, G., Vivekanand and Kherb, J., 2026. Thermogravimetric analysis and determination of kinetic parameters for pyrolysis of lotus seed biomass. *Nature Environment and Pollution Technology*, 25(3), B4389. https://doi.org/10.46488/NEPT.2026.v25i03. B4389

Note: From 2025, the journal has adopted the use of Article IDs in citations instead of traditional consecutive page numbers. Each article is now given individual page ranges starting from page 1.

1. INTRODUCTION

With growing instances of climate change-induced environmental issues and a continuous lookout for sustainable energy solutions, omnipresent and highly abundant biomass is a flicker of hope. It is primarily derived from various agricultural byproducts. Usage and proper processing of this vast resource may hold the key to unlocking a great renewable energy option. The current global economic development is mostly based on trade and processing of crude oil whose continuous depletion is seen as both economic and energy supply problem since energy demand is exponentially increasing (Jankovic et al. 2020) Additionally, combustion of these fossil fuels leads to release of harmful gases like carbon, nitrogen and sulfur oxides in the environment which results in respiratory problems in living beings (Kampa & Castanas 2008). Many of these pollutant gases also have a prominent greenhouse effect, thereby leading to an increase in Earth's temperature. In such an alarming situation, the effective usage of Biomass as a renewable energy is a highly plausible option. Utilization of biomass will also conform to the globally accepted environmentally sustainable practices. Currently, hydrogen gas fuel is generated mostly from the usage of fossil fuels, which also releases CO_2 (Muradov & Veziroglu 2008). Biomass seems to be a good alternative to fossil feedstocks in this regard as well due to its zero net CO_2 impact (Francis Prashanth et al.

2020). From an energy generation point of view, plant as well as animal-based biomass material have been found highly useful (McKendry 2002). Additionally, Biomass is a type of easily biodegradable organic material, making it environmentally compatible as well. Most commonly seen biomass in our surroundings includes crop leftovers, millions of tonnes of leaves/branches/barks emanating from forest plants/trees, municipal waste generated primarily by large urban areas, and waste products released by some industries such as food packaging firms. Biomass also includes gases and liquids recovered from the decomposition of non-fossilized and biodegradable organic materials. As the Earth contains millions of plant and animal species, there is a diverse variety of biomass available, and researchers have minutely studied the composition and unique aspects of many biowaste materials, such as banana peel, apple pomace, and coconut shell, to name a few. One of the highly abundant plant varieties in India is the lotus and its variants. Lotus is an aquatic flowering plant that grows in nutrient-rich freshwater. It comes from the plant family of Nelumbonaceae, and it is also regarded as a sacred flower across many parts of the world (Premathilake & Seneviratne 2015). All parts of this plant species are utilized as food and medicine (Mukherjee et al. 2009). The lotus plant doesn't require specific growing conditions, and that's why it is found in a wide variety of climates ranging from South America to Russia and everywhere in between (Dumont 1995). Lotus seed (LS) is an incredibly significant part of the lotus plant due to its high nutritional value as well as the bioactive nature of its components. Specifically, the presence of phenolic compounds in LS extracts imparts anti-cancer, anti-proliferation, anti-diabetic, anti-inflammatory, neuroprotective, antioxidant, and immunomodulatory responses in therapeutic applications (Zhao et al. 2014). Utilizing such easily available, nutrient-rich, economical horticultural waste for producing value-added products will be an excellent step towards sustainable utilization goals. Lotus seeds, despite their small and compact size, are rich in nutrients, including proteins, vitamins, and essential minerals like magnesium, potassium, and phosphorus (Zhu 2017). Their usage is also rather easy, as they can be consumed in raw form, roasted form, or cooked form. Recent studies have shown that their continuous consumption leads to significant enhancement in good health parameters in human beings, such as improved sleep quality and lowered aging-related ailments (Zhang et al. 2015). They also have high cultural and historical significance as they symbolize purity, rebirth, and enlightenment in many countries (Yang et al. 2024). When stored properly, they have a long shelf life. Among a diverse variety of biomass resources available on earth, lotus seeds are not only abundant but also possess a unique chemical composition, thereby making them an intriguing avenue for further research and exploration studies. Lotus seeds are mostly sold in dried, shelled form, which is called "Makhana" (Arooj et al. 2021). Makhana, derived from lotus seed, is rich in nutrients. Its ease of processing and workability make it a promising research target for potential applications such as energy generation through pyrolysis. Pyrolysis is a thermochemical conversion that has the power to unlock the energy potential that is embedded in the lotus seeds. The lotus seeds' biomass is subjected to controlled heat in an oxygen-deficient environment, and valuable products like biochar and bio-oil can be obtained (Hou et al. 2021). Therefore, using the process of pyrolysis leads to optimization of energy and environmentally sustainable usage of biomass (Müller-Hagedorn & Bockhorn 2007). Pyrolysis data of such biowastes is highly informative, as the intermolecular forces of the constituent species invariably dominate this thermal process. Therefore, the determination of the different parameters obtained from theoretical modeling of pyrolysis data provides key information about the underlying chemical reactions as well as the structure and composition of this material.

This research work is focused on detailed elemental and thermochemical profiling of lotus seed biomass, which has been missing in previous studies. Thermogravimetric analysis of lotus seeds was systematically carried out at varying heating rates, and the associated thermochemical changes were correlated to compositional changes in the material. Judicious utilization of such information regarding lotus seeds not only solves the biomass pollution problem but also provides a viable energy alternative, thereby leading to sustainable living practices. Thermo-chemical conversion processes primarily use heat or chemicals to convert biomass into another usable chemical form (Demirbas 2001). In this regard, the most commonly used techniques include gasification, combustion, and pyrolysis. These techniques differ from each other principally by the extent to which the chemical reactions involved are allowed to proceed. Herein, we have focused on the pyrolysis technique to study the thermal changes in LS biomass. Pyrolysis is a thermochemical decomposition of organic or inorganic material at very high temperatures in the absence of oxygen (Bridgwater 2012). It involves a simultaneous gradual change of elemental composition and physical phase in the material subjected to high temperature exposure. In the case of biomass, this process generally entails thermally driven breaking of the complex cellulosic structure to simpler molecular fragments rich in carbon, oxygen, and hydrogen (Noszczyk et al. 2021). The lower molecular weight compounds remain as permanent gases at ambient temperature, while the majority of complex, larger compounds condense to form a liquid, which is called

bio-oil (Mohan et al. 2006). Before the emergence of the petrochemical industry, a number of useful products such as methanol, phenols, carboxylic acids, and furfural were derived from the pyrolysis of liquids generated during charcoal manufacturing (Basu 2013). After the realization of limited sources of fossil fuels across the globe and their adverse impacts on the environment, the use of biomass as a source of energy has again seen renewed interest since the 1990s. The bio-oil has also been used as a fuel in a diesel engine with slight modifications in the fuel pump, engine linings, and cylinder-injection system (Hall & Scrase 1998). They can also be used in simple oil burners for thermal applications and in combustion boilers to generate electricity, or can be easily blended with standard diesel fuels to form a pollution-free green bio-diesel fuel (Atabani et al. 2013). The bio-oil also has good potential as a chemical feedstock, which is mainly controlled by the availability of oxygen and conversion temperature (Guerrero et al. 2014). Additionally, in this work, we have investigated the thermodynamic and kinetic parameters of the pyrolysis process using various theoretical models. Kinetic factors involved in thermal decomposition reactions primarily regulate the conversion process of biomass into desirable final energy products (Ma et al. 2017). Accurate kinetic models are therefore needed for the most effective utilization of particular biomasses and for scaling up to real industrial applications for energy generation purposes (Huang et al. 2016). A complete understanding of process kinetic parameters helps in getting proper control and optimization of biomass thermal treatment. These kinetic parameters generally include activation energy (E_a), pre-exponential factor (A), the reaction rate constant (k), and the reaction order (n). Improved knowledge of these parameters enables modeling, designing, and optimization of bioreactors for biomass pyrolysis.

2. MATERIALS AND METHODS

2.1. Preparation and Collection of Raw Material

The sample *Nelumbo nucifera* (lotus seeds) was collected from seed pods of the lotus plant located in Gadarpur, Uttarakhand, India, and ground into fine powder form before its pyrolysis and other chemical analysis.

2.2. *Nelumbo nucifera* (Lotus Seeds) Powder Preparation

The collected seeds were kept in a hot air oven at 60°C for 2 hours to remove the majority of their moisture content. Thereafter, the dried seeds were powdered using a grinding machine and then sieved using a laboratory sieve of mesh 100 (149 microns pore size) to finally obtain solid, homogeneous contents with uniform particle size.

2.3. Characterization of Raw Material

2.3.1. Proximate Analysis

The percentage moisture content of the sample was determined by heating the samples in a pre-weighed pan. The samples were then dried at 100°C in accordance with ASTM D3173 standards. The percentage moisture content in the tested biomass was calculated using the following equation (Jo et al. 2017).

$$\%\ Moisture\ Content = \frac{(Wet\ weight - Dry\ Weight)}{Wet\ weight} \times 100 \quad \ldots(1)$$

Thereafter, the same heated sample was kept in a muffle furnace at 1000°C for 5 minutes. This treatment led to the softening of the solid sample and the removal of trapped volatile gases such as carbon dioxide and methane from it. The resulting ash-like material was weighed after cooling to room temperature. The volatile matter content was then calculated using the following equation:

$$\%\ Volatile\ Matter\ Content = \frac{(Weight\ of\ dry\ sample - Ash\ Weight)}{Dry\ sample\ weight} \times 100 \quad \ldots(2)$$

Ash content of the wastes refers to the non-combustible material left after the biowaste is completely burned at 700°C for 1 hour in the presence of air. Thereafter, the fixed carbon percentage in the biomass sample was computed by subtracting the mass of volatiles, moisture, and incombustibles from the original mass of the sample, using the following equation:

$$\%\ Fixed\ carbon\ Content = 100 - (\%\ Moisture + \%\ Ash + \%\ Volatile\ matter) \quad \ldots(3)$$

2.3.2. Ultimate Analysis

This is a chemically more specific and accurate method for determining the elemental composition of the material, usually focusing on C, H, N, S and O content of the sample. This includes the determination of the exact chemical form of sulfur present; the most common forms are in the form of sulfide minerals, sulfate minerals, or organically bound sulfur. In some cases, the analyses might reveal the presence of other important trace elements that may influence the suitability of the material for a particular purpose.

Ultimate analysis of the powdered sample was carried out using a CHNSO elemental analyzer (Elementar Analysensysteme Germany, Model: Vario Micro Cube), which provided % composition of C, H, N, S and O in the sample. This machine has a combustible working temperature range of 950-1200°C. During this simultaneous detection of elements in the feed sample, helium gas was used as the carrier gas.

2.4. Spectral Characterization of Raw Biomass Material

FTIR spectra of the powdered and pyrolyzed samples were used for detailed functional groups analysis. The Agilent Cary 630 FTIR spectrometer was used for the analysis in the spectral range of 450-4000 cm^{-1}. Before FTIR analysis, samples were heated at two distinct temperatures, i.e., 550°C and 1000°C, so that thermally induced chemical changes in samples can be carefully observed vis-à-vis the changes in functional groups' spectral features. The raw powdered biomass of the lotus seed sample was carefully placed in a quartz crucible, and it was first subjected to 550°C. This was followed up by heating the raw sample even further at 1000°C in a quartz crucible. Samples were then kept at room temperature to cool down before the collection of FTIR data. FTIR spectra of the untreated biomass sample and the thermally treated samples were collected via traditional KBr pellet methodology.

2.5. Thermal Characterization of Raw Material

The detailed thermal profiling of the sample was performed using simultaneous TGA-DTG-DTA and DSC analysis on an EXSTAR TG/DTA 6300 instrument. The analysis was performed at three different heating rates of 5°C.min^{-1}, 10°C.min^{-1}, and 20°C.min^{-1}, with alumina as a reference in an inert N_2 atmosphere at a flow rate of 200 mL.min^{-1}. Approximately 10 milligrams of finely powdered sample was subjected to gradually heating program to a final temperature of 1000°C. The thermogravimetric (TG) data were minutely studied to calculate ash yield, thermal stability, and % weight residue loss in the samples at different temperatures.

2.6. Theoretical modeling of TGA data

Detailed thermodynamic and kinetic modeling of the obtained thermogravimetric data has been carried out to understand the thermal-induced changes in the sample. TGA data for each biomass sample were analyzed to assess their weight loss (%) in relation to temperature, decomposition stages, and kinetic parameters. These analyses were performed through a set of calculations using well-accepted theoretical models of Coats and Redfern (CR) and Ozawa-Flynn-Wall (OFW). Origin® software from OriginLab® Corporation was used for equation fitting and regression analysis of the data.

2.7. Evaluation of Thermodynamic Parameters

Each TGA curve was subdivided into five phase stages to evaluate the frequency factor (A), activation energy (E_a), change in entropy (ΔS), change in enthalpy (ΔH), and change in free energy (ΔG) associated with these thermally induced chemical reactions through the following equations:

$$\Delta H = E_a - RT_p \quad \ldots(4)$$

$$\Delta G = E_a + RT_p \ln\frac{k_b T_p}{hA} \quad \ldots(5)$$

$$\Delta S = \frac{\Delta H - \Delta G}{T_p} \quad \ldots(6)$$

$$\Delta A = [\beta exp(E_a/RT_{max})E_a]/(RT_{max}^2) \quad \ldots(7)$$

Where the involved symbols have their usual meaning (R being the ideal gas constant having a value of 8.314 J $mol^{-1}K^{-1}$, T_p is peak decomposition temperature in K, k_b is the Boltzmann constant having a value of 1.38×10^{-23} J K^{-1}, h is Planck's constant with a value of 6.63×10^{-34} Js)

2.7.1. Coats and Redfern (CR) Model

The Coats-Redfern model is a widely used method in thermal analysis, particularly in the study of reaction kinetics for solid-state processes such as the decomposition of material (Álvarez et al. 2016). The CR model was applied to find out the non-isothermal kinetics and thermodynamic parameters from the collected TG data. The CR method involves constructing a plot of $[\log_{10}(1-\alpha/T^2)]$ vs. T^{-1} wherein the slope of the straight line w $-E_a/2.303R$ It can be utilized for finding the activation energy of the process.

$$\ln[g(\alpha)] = -\frac{E_a}{RT} + \ln\left(\frac{AR}{\beta E_a}\right) \quad \ldots(8)$$

Where $g(\alpha) = -ln\left[\frac{1-\alpha}{T^2}\right]$ for $n = 1$ and

$g(\alpha) = \frac{1-(1-\alpha)^{1-n}}{(1-n)T^2}$ for $n \neq 1$

2.7.2. Ozawa-Flynn-Wall (OFW) Model

The OFW model, also known as the Ozawa-Flynn-Wall (OFW) method, is used in thermal analysis to find the activation energy of a reaction without even having intricate knowledge of the reaction mechanism (Flynn & Wall 1966). It is particularly used for the study of solid-state reactions, such as the thermal decomposition of materials.

The OFW model basically correlates the heating rate of the samples with the activation energy associated with processes, utilizing Doyle's approximation for the temperature integral. The final form of the OFW equation is expressed as follows:

$$\log(\beta) = \log\left[\frac{AE_a}{Rg(\alpha)}\right] - 2.315 - 0.457\,\frac{E_a}{RT} \quad \ldots(9)$$

As can be seen from the OFW equation, a linear plot of log β versus 1/T is adequate to determine the activation energy for each conversion step.

2.8. Evaluation of Kinetic Parameters

Thermal degradation refers to the process in which a

material's chemical structure breaks down when it is gradually exposed to elevated temperatures. This breakdown often leads to a significant loss of physical/chemical properties, changes in visual appearance, and the release of volatile compounds. The overall rate equation for the pyrolysis of solid biomass can be expressed as a function of conversion α, as follows:

$$\frac{d\alpha}{dt} = k(T)f(\alpha) \quad \ldots(10)$$

Conversion (α) is a type of weight loss data of a decomposed sample and is defined as follows:

$$\alpha = \frac{m_i - m_a}{m_i - m_f} \quad \ldots(11)$$

Wherein m_i is the initial weight of the biomass sample at temperature, mt is the weight of the biomass sample at time t, and mf is the final weight of the biomass sample at the end of the thermal degradation process.

The rate constant k (T) for this solid-state reaction can be expressed by the Arrhenius relation as:

$$k = Ae^{\left(\frac{-E_a}{RT}\right)} \quad \ldots(12)$$

Substituting the value of k in equation (10),

$$\frac{d\alpha}{dt} = A.f(\alpha).e^{-E_a/RT} \quad \ldots(13)$$

Since temperature T depends upon time, the heating rate term β can be defined as:

$$\beta = \frac{dT}{dt} = \frac{d\alpha}{dt} \quad \ldots(14)$$

Substituting the heating rate formula in equation (13) leads to:

$$\frac{d\alpha}{dt} = \frac{A}{\beta}.(1-\alpha)^n.e^{-Ea/RT} \quad \ldots(15)$$

The integration of the above equation within the limits α = 0 to α and T = 0 to T gives:

$$g(\alpha) = \int_0^\alpha \frac{d\alpha}{f(\alpha)} = \frac{A}{\beta}\int_0^T exp\left(\frac{-E_a}{(RT)}\right)dT \quad \ldots(16)$$

where g(α) represents the integral reaction model. This equation can be solved for E_a (activation energy) and A (pre-exponential factor) using model-free and reaction-fitting methods.

Equation (16) on integration and further simplification gives,

$$ln\frac{g(\alpha)}{T^2} = ln\frac{AR}{\beta E_a} - \frac{E_a}{RT} \quad \ldots(17)$$

A plot of ln[G(α)]/T² versus 1/T yields a straight line with slope $-E_a/R$ and an intercept corresponding to ln(AR/βE). The functions G(α) and F(α) are determined by the mathematical model describing the thermochemical conversion mechanism. For the pyrolysis of the sample, the appropriate kinetic model is identified through linear regression analysis. The plot of ln[G(α)]/T² versus 1/T should exhibit a straight line with a correlation coefficient (r^2) close to 1, indicating the best-fit kinetic model.

To find out the kinetic parameters, eight kinetic models were adopted to study the thermal decomposition of biomass samples. The degradation process of the biomass is overall influenced by transport (diffusion) phenomena and chemical reaction kinetics. Different algebraic expressions were used to identify the reaction mechanisms in thermochemical decomposition reactions (Malika et al. 2016). These expressions have been listed in Table 1.

2.9. SEM Analysis

Scanning Electron Microscopy is a powerful visualization technique used to examine the surface structure and

Table 1: Algebraic equations employed for the determination of reaction kinetic mechanisms and parameters.

Mechanism		Symbol	$f(\alpha)$	$g(\alpha)$
Chemical reaction kinetics	First order	F_1	$1-\alpha$	$-\ln(1-\alpha)$
	Second order	F_2	$(1-\alpha)^2$	$(1-\alpha)^{-1}-1$
	Third order	F_3	$(1-\alpha)^3$	$[(1-\alpha)^{-2}-1]/2$
Diffusion kinetics	One-way transport	D_1	$1/2\,\alpha$	α^2
	Two-way transport	D_2	$-\ln(1-\alpha)^{-1}$	$\alpha+(1-\alpha)-\ln(1-\alpha)$
	Three-way transport	D_3	$\frac{\left(\frac{2}{3}\right)(1-\alpha)^{2/3}}{1-(1-\alpha)^{1/3}}$	$[1-(1-\alpha)^{\frac{1}{3}}]^2$
	Ginstling, Brounshtein equation	D_4	$\frac{\left(\frac{2}{3}\right)(1-\alpha)^{1/3}}{1-(1-\alpha)^{1/3}}$	$1-\frac{2\alpha}{3}-(1-\alpha)^{2/3}$
	Zhuralev, Lesokhin, Tempelman Equation	D_5	$\frac{\left(\frac{2}{3}\right)(1-\alpha)^{5/3}}{1-(1\alpha)^{1/3}}$	$[(1-\alpha)^{\frac{1}{3}}-1]^2$

Table 2: Proximate analysis data of the LS biowaste sample.

Proximate Analysis	LS parameters	% w/w
	Moisture content	5.77
	Volatile matter	76.3
	Fixed carbon	15.56
	Ash content	2.37

composition of materials at very high magnifications. SEM images for three different samples, i.e., raw sample and samples treated at 550°C and 1000°C were taken using a JEOL Japan model JSM 6610V microscope using a tungsten or LaB6 filament, which provided detailed images of the sample surface by scanning it with a focused beam of electrons. High-resolution microscopic imaging of samples under different conditions helped in the proper understanding of the physical and structural aspects of biomass and the nature of its thermal transformation process.

3. RESULTS AND DISCUSSION

3.1. Proximate Analysis

A known quantity of LS biowaste was subjected to distinct heating steps, and subsequent weight losses in the sample were correlated with important fuel parameters present in the sample. The obtained results have been summarized in Table 2.

From the observed data, it can be concluded that LS biowaste contains a very small amount of moisture and ash content. These traits certainly enhance its potential utilization as an energy material.

3.2. Ultimate Analysis

Ultimate analysis of the LS (Lotus Seed) sample was performed using a Vario micro cube CHNS analyzer. Results have been summarized in Table 3. From the data, it was clearly observed that the tested sample was rich in carbon and contained 39.66 % carbon, 5.842% hydrogen, 8.166 % nitrogen, and 1.397% of sulphur. Oxygen content was determined by adding all the elements and subtracting it from 100. Thereafter, Oxygen content was found to be 44.935%, making it the most abundant element in this biomass sample.

Furthermore, Gross Calorific Value (GCV) and Net Calorific Value (NCV) for the LS biowaste sample can be easily calculated using CHNS data (Elkhalifa et al. 2022).

The GCV includes the latent heat of steam condensation. It can be mathematically calculated by using elemental percentages in equation (18).

Table 3: Ultimate analysis data of the LS biowaste sample.

Ultimate Analysis	Element	Amount in LS sample %
	Carbon	39.66
	Hydrogen	5.842
	Nitrogen	8.166
	Sulphur	1.397
	Oxygen	44.935
	C/N ratio	17.536
	C/H ratio	6.788

$$GCV\ (kJ.kg^{-1}) = 349.1\ C + 100.5\ S + 1178.3\ H - 103.4\ O - 15.1\ N - 21.1\ Ash \quad \ldots(18)$$

GCV value for the analyzed LS sample was found to be 16049.74 ($kJ.kg^{-1}$)

Similarly, Net calorific value, which excludes the latent heat of steam condensation, can be computed by using equation (19).

$$NCV\ (kJ.kg^{-1}) = GCV - H_{st}\ (0.09\ H + 0.01\ M) \quad \ldots(19$$

where H_{st} denotes the enthalpy of steam (2260 $kJ.kg^{-1}$), and M denotes the moisture (%) in the fuel sample.

Net calorific value for the LS sample was found to be 14732.838 ($kJ.kg^{-1}$).

3.3. FTIR Analysis

FTIR spectra of raw LS sample and pyrolyzed LS samples were collected to delve into functional group changes in the biomass during the thermal treatment. The obtained spectra are shown in Fig. 1. All three samples showed a prominent broad spectral feature in the range ~ 3400 cm-1 to 3200 cm-1, which is generally attributed to the H-bonded O-H group of cellulose (Grube et al. 2006). The band at 2930 cm^{-1} can be ascribed to C-H stretching of the methylene group of cellulose (Peng et al. 2010). This spectral feature became very weak at 500°C and became negligible at 1000°C, indicating significant loss of carbon content as pyrolysis proceeds. Raw sample also showed a strong peak at 1659 $cm^{-1,}$ which may be assigned to conjugated -C=O stretching. Spectral feature at 1549 cm^{-1} indicates the presence of -C=C- conjugated with aromatic rings in the biomass. The absorption peaks at 1246 cm^{-1} and 1155 cm^{-1} can be attributed to stretching of -C-O-C- ether linkages prevalent in guaiacyl lignin and aromatic C-H deformations (Zhong et al. 2007). These peaks vanished for pyrolyzed samples, which indicates the breakdown of ring structure in this lignocellulosic biowaste. Multiple weak bands in the 500-900 cm-1 region are due to C-H bending vibrations in olefinic or aromatic contents. Even these spectral features became weaker as biowaste was treated at high temperatures.

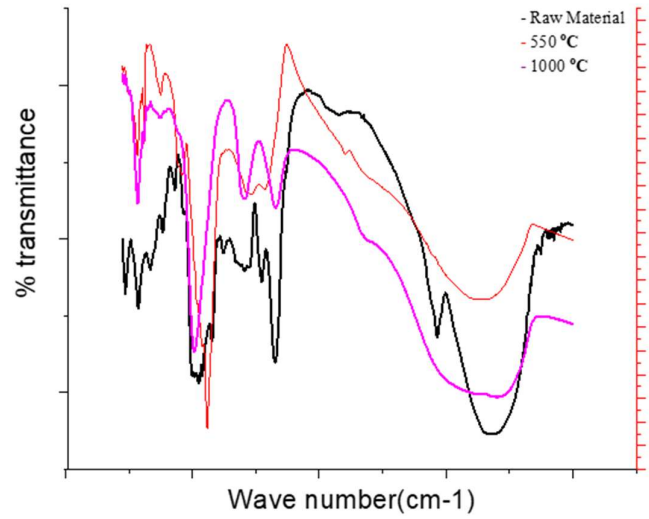

Fig. 1: FTIR spectra of Raw LS sample, after 550°C treatment and after 1000°C treatment.

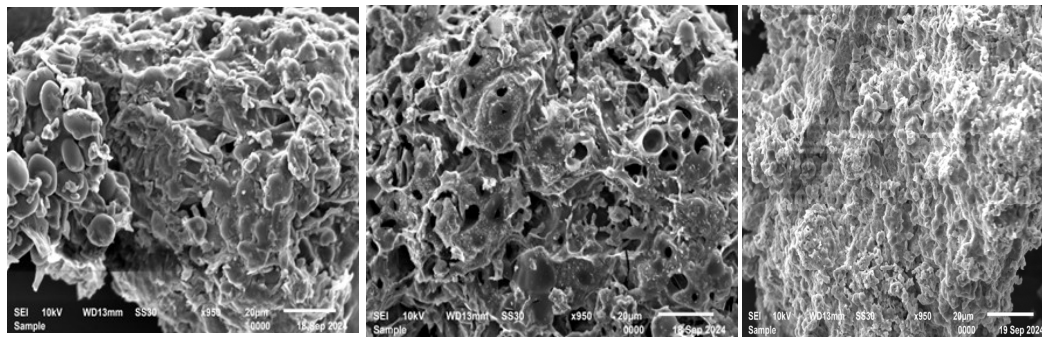

Fig. 2: SEM image of: (a) Raw LS sample, b) Sample after 550°C treatment and c) 1000°C treatment.

Overall, intensities of typical lignin-associated spectral features clearly became weaker during the high-temperature thermal treatment of the LS sample.

3.4. SEM Analysis

SEM images of the LS powdered sample were taken before and after pyrolysis treatment at 550 and 1000 degree Celsius. Collected images are shown in Fig. 2. As can be clearly seen, large-scale structural disintegration was observed in the sample after high-temperature exposure. Sample treated at 550°C showed a considerable amount of porosity, which can be attributed to loss of volatile gases from soft lignocellulosic biomass (Zhang et al. 2020 & Calin et al. 2024). This also correlates well to FTIR spectral changes, indicating a high degree of loss of - C=O, -C-O-C- and -OH functionalities from the biomass. Further increase in pyrolysis temperature led to compaction in the treated biomass. This can be explained by the loss of lignocellulosic content from the LS sample.

3.5. Thermal Analysis of LS Biomass

The thermal analysis of each biomass type was carried out at 3 different heating rates of 5°C.min^{-1}, 10°C.min^{-1} and 20°C.min^{-1} in an inert N_2 atmosphere with a flow rate of 200 mL.min^{-1}. The results obtained were then analyzed to compare the thermal degradation of lignocellulosic biomass under the same heating conditions. The TGA as well as DTG results for three heating rates have been shown in Fig. 3. Recorded TGA curves displayed an overall sigmoidal shape, while the DTG curves exhibited two or three major peaks.

The TGA and DTG curves for biomass LS exhibited a pronounced peak for significant weight loss between 70°C and 100°C, indicating the loss of moisture and other volatile substances. The effect of heating rate on the same biomass types was also observed during the moisture removal stage. At a heating rate of 5°C.min^{-1}, there was 8.52% weight loss due to the loss of moisture and other volatiles. This weight loss decreased to 7.75% at a heating rate of 10°C.min^{-1}, and then decreased to 6.92% at a heating rate of 20°C.min^{-1}.

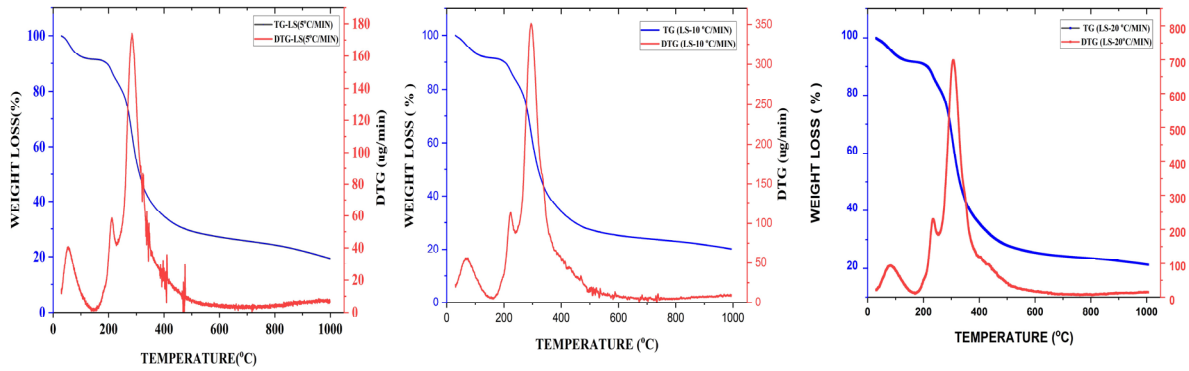

Fig. 3: TGA and DTG Curves of LS biomass at a heating rate of 5°C.min^{-1}, 10°C.min^{-1}, and 20°C.min^{-1}

The DTG curves in Fig. 3 show that the primary pyrolysis decomposition at all rates of biomass LS occurred approximately between 200°C and 400°C. Cellulose, being a homogeneous semi-crystalline polymer of glucose units, degrades within a narrow temperature range. Its decomposition extends up to around 400°C, where the main devolatilization reactions occur. This marks the active pyrolysis stage, characterized by a significant release of volatile matter (VM).

The thermal decomposition of these biomasses is influenced by their lignocellulosic components (hemicellulose, cellulose, and lignin), which typically decompose over the temperature range of 200-400°C (Weerachanchai et al. 2010). Lignin generally begins decomposing at the lowest temperature and continues up to around 900°C. Hemicellulose and cellulose decompose over the temperature ranges of 160-360°C and 240-390°C, respectively (Vamvuka et al. 2003).

Pyrolysis at higher heating rates resulted in a faster decomposition rate, and a broader temperature range was seen for thermal decomposition. The pyrolytic breakdown of hemicellulose and cellulose primarily accounts for the second DTG peak. At a pyrolysis temperature of 241°C, the LS residue showed the highest derivative weight loss. This suggests that LC-BM residue may contain larger fractions of cellulose and hemicellulose, contributing to the release of more volatile components. In contrast, LS biomass likely contains very little lignin content, as there is no indication of any derivate peak after 600°C.

In LS, no significant peak after 600°C in the DTG curve was observed at any heating rate, indicating that lignin content was quite low because the lignin degradation began at 180°C and continued until 950°C, occurring over a wide temperature range as a distinct pyrolytic process. The absence of lignin at a later stage indicates that the biomass LS is not thermally stable above the temperature range of 600°C due to the absence of much lignin, resulting in the absence of its polyaromatic structure. This stage only corresponds to the formation of ash and the burning of fixed carbon content. It is evident that the devolatilization region of biomass LS shifts within the range of 120°C to 600°C due to varying heating rates (5°C.min^{-1}, 10°C.min^{-1}, and 20°C.min^{-1}). This shift is attributed to internal factors or biochemical interactions and synergistic effects that occur during the thermal decomposition of lignocellulosic biomass.

3.6. Evaluation of Thermodynamic Parameters

Employing the CR model, the values of $1/T$ and $ln[-ln(1-X)]$ were calculated and plotted from the TGA data by splitting the entire thermal range into five phases to obtain different thermodynamic parameters including frequency factor (A), activation energy (E_a), change in entropy (ΔS), change in enthalpy (ΔH) and change in free energy (ΔG). This was done for the LS samples at three different heating rates of 5°C.min^{-1}, 10°C.min^{-1}, and 20°C.min^{-1}. Similarly, for the OFW model, data between $ln\beta$ $vs.1/T$ were plotted to calculate the slope, which in turn provided the values of the above-mentioned thermodynamic parameters. All of the obtained thermodynamic parameter values from both models have been summarized in Table 4.

As can be seen from the observed results, the activation energies obtained from both CR and OFW models were of similar order. Entropy change (ΔS) calculated using both models across was found to be negative across five phases, indicating that the disorder of the products after bond dissociation was lower than that of the initial reactants. This negative ΔS suggests that the intermediate state formed during thermal degradation had a more structured and organized arrangement as compared to the chemical bonding in the raw LS sample. Gibbs free energy change generally reflects the absolute energy increase during any reaction process and formation of the activated complex. Higher ΔG values computed here clearly indicate reduced spontaneity of the pyrolysis reactions of this biowaste sample. Using

Table 4: Thermodynamic parameters for LS thermal degradation computed with CR and OFW models.

HEATING RATE	PHASE	ISOCONVERSIONAL METHODS									
		CR MODEL					OFW MODEL				
		E_a [kJ.mol^{-1}]	A [sec^{-1}]	ΔH [kJ.mol^{-1}]	ΔG [kJ. mol^{-1}]	ΔS [kJ. mol^{-1}]	E_a [kJ. mol^{-1}]	A [sec^{-1}]	ΔH [kJ. mol^{-1}]	ΔG [kJ. mol^{-1}]	ΔS [kJ. mol^{-1}]
5°C.min^{-1}	100	2.79	0.013	-0.31	117.8	-316.7	2.79	0.183	-0.31	96.9	-260.8
	200	3.49	0.010	-0.44	151.1	-320.4	3.48	0.178	-0.44	12.3	-263.0
	300	4.32	0.011	-0.43	184.3	-321.6	4.32	0.187	-0.43	15.0	-264.2
	500	5.53	0.010	-0.89	251.2	-325.0	5.53	0.168	-0.89	20.5	-267.6
	900	7.90	0.009	-0.18	386.4	-329.4	7.90	0.150	-0.18	31.7	-272.0
10°C.min^{-1}	100	2.783	0.00043	-0.317	115.6	-311.0	2.78	0.365	-0.31	94.8	-255.1
	200	3.489	0.00035	-0.443	148.4	-314.7	3.49	0.357	-0.44	12.1	-257.2
	300	4.329	0.00037	-0.434	180.5	-315.9	4.32	0.374	-0.43	14.7	-258.4
	400	5.532	0.00033	-0.893	245.9	-319.2	5.53	0.337	-0.89	20.1	-261.8
	500	7.908	0.00030	-0.184	377.8	-323.7	7.90	0.300	-0.18	31.0	-266.2
20°C.min^{-1}	100	2.770	0.00087	-0.330	113.5	-305.2	2.77	0.724	-0.33	92.7	-249.4
	200	3.491	0.00085	-0.440	144.9	-307.4	3.49	0.716	-0.44	11.8	-251.5
	300	4.330	0.0007	-0.433	177.2	-310.1	4.33	0.749	-0.43	14.4	-252.7
	400	5.536	0.00067	-0.890	241.4	-313.5	5.53	0.674	-0.89	19.2	-256.0
	500	7.911	0.00060	-0.184	371.1	-317.9	7.91	0.600	-0.18	30.5	-260.5

OFW, for all three heating rates, the ΔG value was found to vary in the range of 110-386 kJ.mol^{-1} for five different phases. These values are of similar order as compared to other reported studies on agricultural biomasses like pea waste, mustard stalk, bamboo, and rice husk (Narnaware et al. 2022 and Jagnade et al. 2023). Thermal degradation was overall dominated by the ΔS component, as ΔH values were found to be negligibly small throughout different phases. Lower activation energies associated with different thermal phases (~ 2-8 kJ.mol^{-1}) coupled with significant ΔG values indicate high bio-energy potential of LS biomass.

3.7. Evaluation of Kinetic Parameters

TGA data were thoroughly studied to determine the kinetic parameters of the thermal degradation of LS biomass. The mathematical fitting of the reaction rate equation was performed using the integral method of the Coats and Redfern model (Álvarez et al. 2016). This method is commonly employed for studying the kinetics of solid material degradation. Eight kinetic models have been examined to analyze the thermal decomposition of biomass samples. Previous studies have indicated that the degradation process of biomass is dominated by transport (diffusion) phenomena and chemical reaction mechanisms (Gil et al. 2010, Vlaev et al. 2003).

To investigate the chemical reaction mechanism, a plot of $\ln[g(\alpha)]/T^2$ versus 1/T was constructed, which yielded a straight line with slope −E/R, while ln(AR/□E) remained nearly constant. The expressions of and depend on the order of the mathematical model for each mechanism of the conversion. The selection of the most suitable model for the pyrolysis of biowaste samples is based on linear regression analysis. In essence, numerator, g open paren alpha close paren end numerator, over cap T squared versus 1 over cap T should give a straight line with a correlation coefficient (R^2) close to 1 for the best fit kinetic model. Algebraic expressions of functions of the most common reaction kinetics, including both chemical reaction mechanisms and diffusion mechanisms involved in thermal degradation of solid-state wastes, are listed in Table 1. The calculated values of R^2 for different heating rates to determine the best fit kinetic models have been summarized in Table 5.

From the kinetics data, it can be clearly seen that, as far as the chemical kinetics mechanism is concerned, LS biomass followed the first-order reaction kinetic mechanism at all three different heating rates of 5, 10, and 20°C.min^{-1}. This order mechanism showed the best-fitting parameter values. For the diffusion kinetics mechanism, LS biomass followed the three-way transport diffusion model (k6) for a heating rate of 5°C.min^{-1}. At heating rates of 10 and 20°C.min^{-1}, it seemed to prefer the Ginstling, Brounstein diffusion model (k_7) better. These models have been previously reported to be most appropriate for describing the thermal degradation of lignocellulosic materials (Gil et al. 2010, Vlaev et al. 2003).

Table 5: Correlation coefficient analysis of various chemical kinetics models and diffusion kinetics models.

Heating Rate	Chemical Kinetic Models			Diffusion Kinetic Models				
	k_1	k_2	k_3	k_4	k_5	k_6	k_7	k_8
5 $^{o}C.min^{-1}$	0.6719	0.6714	0.5412	0.9039	0.8881	0.9162	0.912	0.5092
10 $^{o}C.min^{-1}$	0.7505	0.6318	0.5199	0.8773	0.8603	0.9082	0.9115	0.505
20 $^{o}C.min^{-1}$	0.9793	0.5505	0.4975	0.8465	0.8787	0.8916	0.9059	0.5558

4. CONCLUSIONS

This study underscores the significant potential of lotus seeds (Nelumbo nucifera) as a sustainable biomass resource for energy generation through pyrolysis and as a game-changing biomass resource in the fight against climate change and energy scarcity. Our thermogravimetric analysis revealed crucial insights into the thermal behavior and compositional changes of lotus seed biomass, demonstrating its viability for producing valuable energy products such as bio-oil and biochar. Detailed thermochemical analysis, along with spectral characterization, helped in understanding the chemical changes happening in the sample when it's gradually subjected to high temperatures. Thermodynamic and kinetic parameters, including activation energy and reaction rate constants, associated with the thermal degradation of the LS sample were systematically computed. These parameters are quite essential for optimizing the pyrolysis process, enhancing its overall efficiency, and facilitating future scaling-up of biomass conversion technologies for industrial applications.

By utilizing lotus seeds, an abundant agricultural byproduct, we can not only contribute to reducing waste but also promote a circular economy and sustainable energy practices. This research advocates for further exploration of underutilized biomass resources, encouraging innovation in renewable energy solutions that align with global sustainability goals. The findings pave the way for future studies aimed at improving the efficiency of biomass pyrolysis and expanding the application of lotus seeds and other similar resources in the renewable energy landscape (Zhong et al. 2007).

5. ACKNOWLEDGEMENTS

Authors are highly thankful to the Department of Chemistry, National Institute of Technology, Kurukshetra, India, Amity Institute of Applied Sciences, Amity University Noida and Department of Chemistry, Govind Ballabh Pant University of Agriculture & Technology, Pantnagar, Uttarakhand, India for supporting this work.

6. REFERENCES

Álvarez, A., Pizarro, C., García, R., Bueno, J. L. and Lavín, A. G., 2016. Determination of kinetic parameters for biomass combustion. *Bioresource Technology*, 216, pp.36-43. [DOI]

Arooj, M., Imran, S., Inam-Ur-Raheem, M., Rajoka, MSR., Sameen, A., Siddique, R., Sahar, A., Tariq, S., Riaz A., Hussain, A., Siddeeg, A. and Aadil, RM., 2021. Lotus seeds (Nelumbinis semen) as an emerging therapeutic seed: a comprehensive review. *Food Science and Nutrition*, 9(7), pp.3971-3987. [DOI]

Atabani, A. E., Silitonga, A. S., Ong, H. C., Mahlia, T. M. I., Masjuki, H. H., Badruddin, I. A. and Fayaz, H., 2013. Non-edible vegetable oils: a critical evaluation of oil extraction, fatty acid compositions, biodiesel production, characteristics, engine performance and emissions production. *Renewable and Sustainable Energy Reviews*, 18, pp.211-245. [DOI]

Basu, P., 2013. *Biomass Gasification and Pyrolysis: Theory and Practice*. Academic Press.

Bridgwater, A. V., 2012. Review of fast pyrolysis of biomass and product upgrading. *Biomass and Bioenergy*, 38, pp.68-94. [DOI]

Calin, C., Sirbu, E., Tanase, M., Gyorgy, R., Popovici, D. R. and Banu, I., 2024. A thermogravimetric analysis of biomass conversion to biochar: experimental and kinetic modeling. *Applied Sciences*, 14(21), pp.9856. [DOI]

Demirbas, A., 2001. Biomass resource facilities and biomass conversion processing for fuels and chemicals. *Energy Conversion and Management*, 42(11), pp.1357-1378. [DOI]

Dumont, H. J., 1995. The ecology of the Lotus plant: a review. *Aquatic Botany*, 52(1), pp.3-17.

Elkhalifa, S., Mariyam, S., Mackey, H. R., Al-Ansari, T., McKay, G. and Parthasarathy, P., 2022. Pyrolysis valorization of vegetable wastes: thermal, kinetic, thermodynamics, and pyrolysis analyses. *Energies*, 15(17), pp.1-15. [DOI]

Flynn, J.H. and Wall, L. A., 1966. General treatment of the thermogravimetry of polymers. *Journal of Research of the National Institute of Standards and Technology*, 70A(6), pp.487-523.

Francis Prashanth, P., Midhun Kumar, M. and Vinu, R., 2020. Analytical and microwave pyrolysis of empty oil palm fruit bunch: kinetics and product characterization. *Bioresource Technology*, 310(February), pp.123394. [DOI]

Gil, M. V., Casal, D., Pevida, C., Pis, J. J. and Rubiera, F., 2010. Thermal behavior and kinetics of coal/biomass blends during co-combustion. *Bioresource Technology*, 101(14), pp.5601-5608. [DOI]

Grube, M., Lin, J.G., Lee, P.H. and Kokorevicha, S., 2006. Evaluation of sewage sludge-based compost by FT-IR spectroscopy. *Geoderma*, 130, pp.324-333. [DOI]

Guerrero, M. R. B., Marques Da Silva Paula, M., Zaragoza, M. M., Gutiérrez, J. S., Velderrain, V. G., Ortiz, A. L. and Collins-Martínez, V., 2014. Thermogravimetric study on the pyrolysis kinetics of apple pomace as waste biomass. *International Journal of Hydrogen Energy*, 39(29), pp.16619-16627. [DOI]

Hall, D. O. and Scrase, J. I., 1998. Will biomass be the environmentally friendly fuel of the future? *Biomass and Bioenergy*, 19(3), pp.357-367. [DOI]

Hou, Y., Liang, Y., Hu, H., Tao, Y., Zhou, J. and Cai, J., 2021. Facile preparation of multi-porous biochar from lotus biomass for methyl orange removal: kinetics, isotherms, and regeneration studies. *Bioresource Technology*, 329, pp.124877. [DOI]

Huang, X., Cao, J. P., Zhao, X. Y., Wang, J. X., Fan, X., Zhao, Y. P. and Wei, X. Y., 2016. Pyrolysis kinetics of soybean straw using thermogravimetric analysis. *Fuel*, 169, pp.93-98. [DOI]

Jagnade, P., Panwar, N. L. and Agarwal, C., 2023. Experimental investigation of kinetic parameters of bamboo and bamboo biochar using thermogravimetric analysis under non-isothermal conditions. *Bioenergy Research*, 16, pp.1143-1155. [DOI]

Janković, B., Radojević, M. B., Balać, M. M., Stojiljković, D. D. and Manić, N. G., 2020. Thermogravimetric study on the pyrolysis kinetic mechanism of waste biomass from fruit processing industry. *Thermal Science*, 24(6 part b), pp.4221-4239. [DOI]

Jo, J. H., Kim, S. S., Shim, J. W., Lee, Y. E. and Yoo, Y. S., 2017. Pyrolysis characteristics and kinetics of food wastes. *Energies*, 10(8), pp.1-10. [DOI]

Kampa, M. and Castanas, E., 2008. Human health effects of air pollution. *Environmental Pollution*, 151(2), pp.362-367. [DOI]

Ma, P., Yang, J., Xing, X., Weihrich, S., Fan, F. and Zhang, X., 2017. Isoconversional kinetics and characteristics of combustion on hydrothermally treated biomass. *Renewable Energy*, 114(B), pp.1069-1076. [DOI]

Malika, A., Jacques, N., Jaafar, E. F., Fatima, B. and Mohammed, A., 2016. Pyrolysis investigation of food wastes by TG-MS-DSC technique. *Biomass Conversion and Biorefinery*, 6(2), pp.161-172. [DOI]

McKendry, P., 2002. Energy production from biomass (part 1): overview of biomass. *Bioresource Technology*, 83(1), pp.37-46. [DOI]

Mohan, D., Pittman, C. U. and Steele, P. H., 2006. Pyrolysis of wood/biomass for bio-oil: a critical review. *Energy & Fuels*, 20(3), pp.848-889. [DOI]

Mukherjee, P. K., Mukherjee, D., Maji, A. K., Rai, S. and Heinrich, M., 2009. The sacred lotus (Nelumbo nucifera) - phytochemical and therapeutic profile. *Journal of Pharmacy and Pharmacology*, 61(4), pp.407-422. [DOI]

Müller-Hagedorn, M. and Bockhorn, H., 2007. Pyrolytic behaviour of different biomasses (angiosperms)(maize plants, straws, and wood) in low temperature pyrolysis. *Journal of Analytical and Applied Pyrolysis*, *79*(1-2), pp.136-146.

Muradov, N. Z. and Veziroglu, T. N., 2008. "Green" path from fossil-based to hydrogen economy: an overview of carbon-neutral technologies. *International Journal of Hydrogen Energy*, 33(23), pp.6804-6839. [DOI]

Narnaware, S. L. and Panwar, N. L., 2022. Kinetic study on pyrolysis of mustard stalk using thermogravimetric analysis. *Bioresource Technology Reports*, 17, pp.100942. [DOI]

Noszczyk, T., Dyjakon, A. and Koziel, J. A., 2021. Kinetic parameters of nut shells pyrolysis. *Energies*, 14(3), pp.682. [DOI]

Peng, F., Song, H., Xiang, J., Peisheng, L., Huang, D., Jiang, L., Zhang, A. and Zhang, J., 2010. FTIR study of pyrolysis products evolving from typical agricultural residues. *Journal of Analytical and Applied Pyrolysis*, 88, pp.117-123. [DOI]

Premathilake, R. and Seneviratne, S., 2015. Cultural implications based on pollen from the ancient mortuary complex in Sri Lanka. *Journal of Archaeological Science*, 53, pp.559-569. [DOI]

Vamvuka, D., Kakaras, E., Kastanaki, E. and Grammelis, P., 2003. Pyrolysis characteristics and kinetics of biomass residuals mixtures with lignite⁎. *Fuel*, *82*(15-17), pp.1949-1960.

Vlaev, L. T., Markovska, I. G. and Lyubchev, L. A., 2003. Non-isothermal kinetics of pyrolysis of rice husk. *Thermochimica Acta*, 406(1-2), pp.1-7. [DOI]

Weerachanchai, P., Tangsathitkulchai, C. and Tangsathitkulchai, M., 2010. Comparison of pyrolysis kinetic models for thermogravimetric analysis of biomass. *Suranaree J. Sci. Technol*, *17*(4), pp.387-400.

Yang, H., He, S., Feng, Q., Liu, Z., Xia, S., Zhou, Q., Wu, Z. and Zhang, Y., 2024. Lotus (Nelumbo nucifera): a multidisciplinary review of its cultural, ecological, and nutraceutical significance. *Bioresource and Bioprocessing*, 11, pp.18. [DOI]

Zhang, C., Zhang, Z., Zhang, L., Li, Q., Li, C., Chen, G., Zhang, S., Liu, Q. and Hu, X., 2020. Evolution of the functionalities and structures of biochar in pyrolysis of poplar in a wide temperature range. *Bioresource Technology*, 304, pp.123002. [DOI]

Zhang, Y., Lu, X., Zeng, S., Huang, X., Guo, Z., Zheng, Y., Tian, Y. and Zheng, B., 2015. Nutritional composition, physiological functions and processing of lotus (Nelumbo nucifera Gaertn.) seeds: a review. *Phytochemistry Reviews*, 14(3), pp.321-334. [DOI]

Zhao, H.X., Zhang, H.S. and Yang, S.F., 2014. Phenolic compounds and its antioxidant activities in ethanolic extracts from seven cultivars of Chinese jujube. *Food Science and Human Wellness*, *3*(3-4), pp.183-190.

Zhong, X., Wang, Q., Jiang, Z., Yang, X. and Ji, Y., 2007. Enzymatic hydrolysis of pretreated soybean straw. *Biomass and Bioenergy*, 31, pp.162-167. [DOI]

Zhu, F., 2017. Structures, properties, and applications of lotus starches. *Food Hydrocolloids*, 63, pp.332-348. [DOI]